NOAA Award Number: NA09OAR4310116
Recipient Name: The University of Rhode Island
Award Period: 08/01/2009 - 07/31/2011
Program Office: OAR Office of Weather and Air Quality (OWAQ)
Project Title: Improving HWRF-GFDN Coupled Models for Transition to Operations
PIs/PDs: Isaac Ginis and Morris Bender
Report Type: Progress Report
Reporting Period: 08/01/2009 - 01/31/2010

Work Accomplishments:

1. Tasks scheduled for Year 1

a) Increasing horizontal grid spacing in GFDN
b) GFDN-WAVEWATCH III coupling
c) Implementation of ASIM into HWRF
d) Implementation of NCODA analysis for ocean initialization in GFDN for the Atlantic basin.

2. Tasks accomplished this period

a) Increasing horizontal grid spacing in GFDN

During this time period we have reconfigured the grid structure in the GFDN model to increase its spatial resolution within the hurricane core region. The model domain consists of a triply nested grid configuration, in which two inner grids are moveable and two-way interactive. The stationary outermost grid spans 75x75º with 1/2º resolution. The middle grid spans 11x11º with resolution 1/6º. The innermost grid spans 5x5º. The GFDN model presently runs operationally at FNMOC with 1/12º resolution for the innermost grid. We have changed this resolution to 1/18º. The time steps for the outer, middle and inner grids have been changed from respectively 60, 30 and 10 seconds to 45, 15 and 5 seconds to satisfy the CFL condition of computational stability. All model code subroutines responsible for coupling between the atmospheric and ocean models have been modified to reflect the changes in the atmospheric grid structure.

To test the high-resolution GFDN system we ran a set of simulations of historic cases in the Atlantic basin. In these simulations we used the GFS analysis for specification of the initial and boundary conditions, similar to the GFDL model run operationally at NCEP (note that the operational GFDN model is run from the NOGAPS analysis). There are also some differences between the model physics of the operational GFDL and GFDN models since some components of the GFDN model physics were upgraded in 2008, while the GFDL model has been frozen since 2007. Figures 1 and 2 show the track and intensity forecasts for Hurricane Katrina (2005) initialized on August 24, 25, and 26 at

00Z using the operational (1/12th degree resolution) version and the high-resolution (1/18th degree resolution) version of the GFDN models. For simplicity, no asymmetries were introduced during the storm bogusing in these simulations. For comparison, we also show the forecasts made by the GFDL operational model. The effect of high resolution is mixed. In two cases, Aug. 24 and Aug. 26, the track forecasts with the high-resolution model were worse that in the operational GFDL model, but significantly improved in the Aug. 25 case. The high resolution model was able to better predict the rapid intensification in the Aug. 25 case (Fig. 2, middle). Figure 3 and 4 show that the vertical and horizontal wind structures are much better resolved in the high-resolution version.

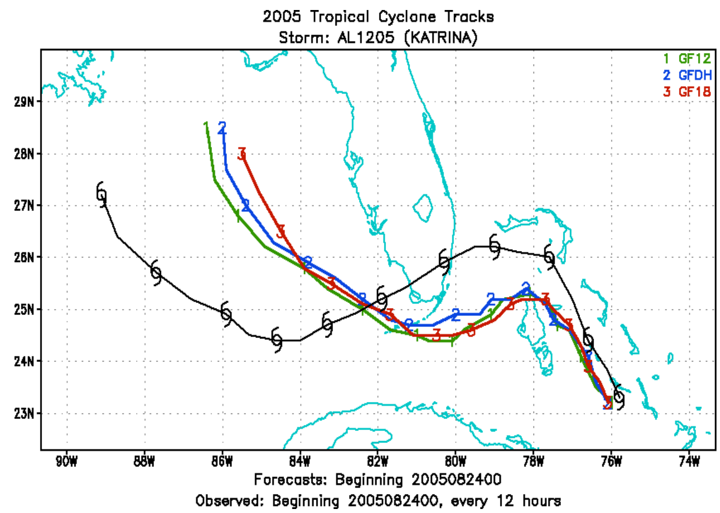

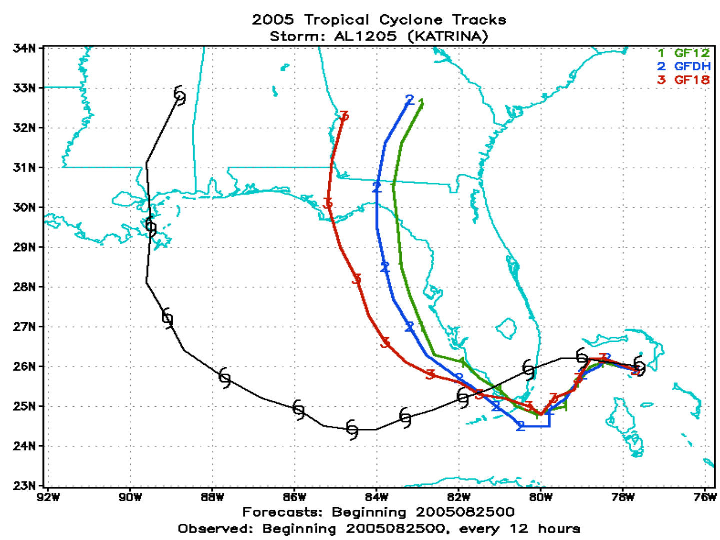

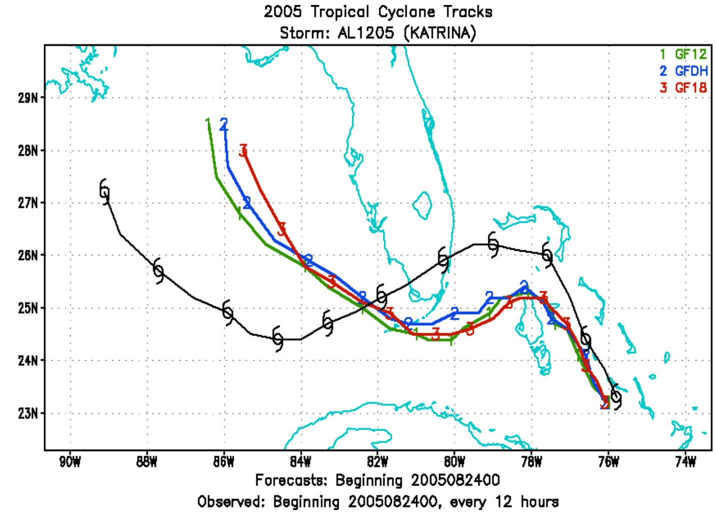

Figure 1. *The tracks simulated by the operational GFDL model (blue), GFDN model (green) and the high-resolution GFDN (red) for Hurricane Katrina (2005) initialized at Aug. 24 00Z (top), Aug. 25 00Z (middle) and Aug. 26 00Z (low).*

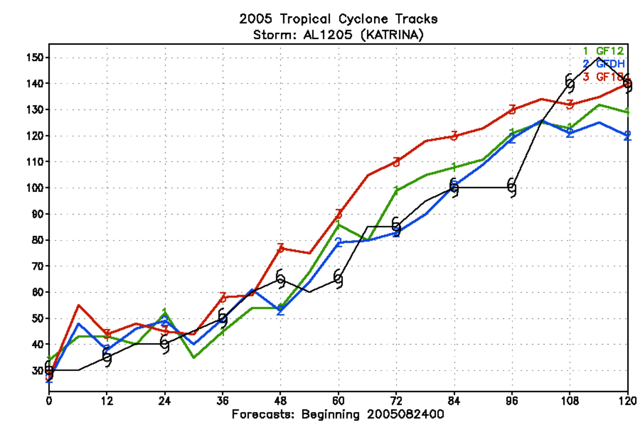

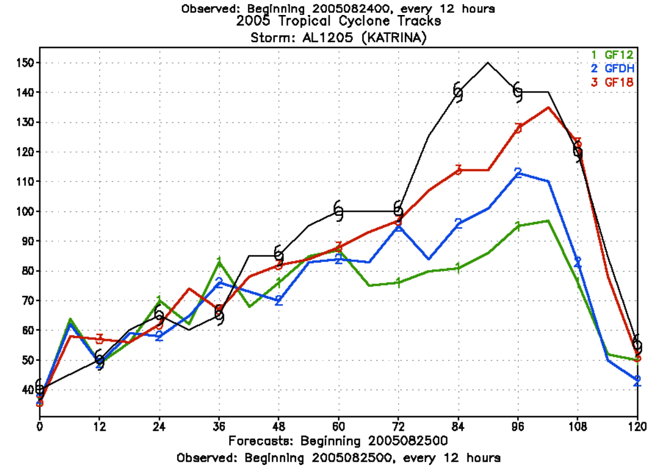

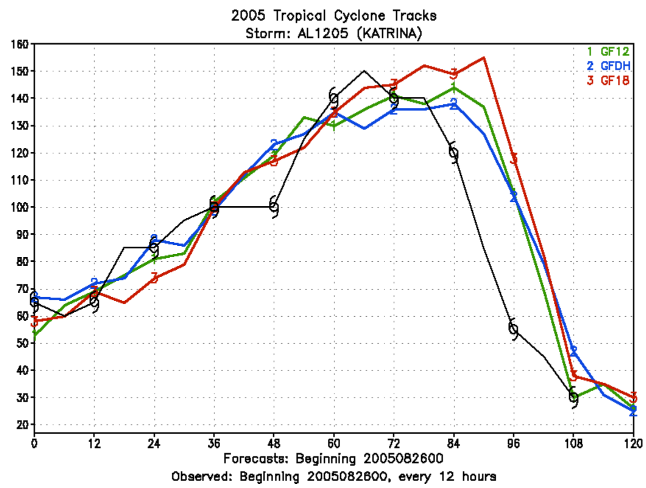

Figure 2. *The maximum winds simulated by the operational GFDL model (blue), GFDN model (green) and the high-resolution GFDN (red) for Hurricane Katrina (2005) initialized at Aug. 24 00Z (top), Aug. 25 00Z (middle) and Aug. 26 00Z (low).*

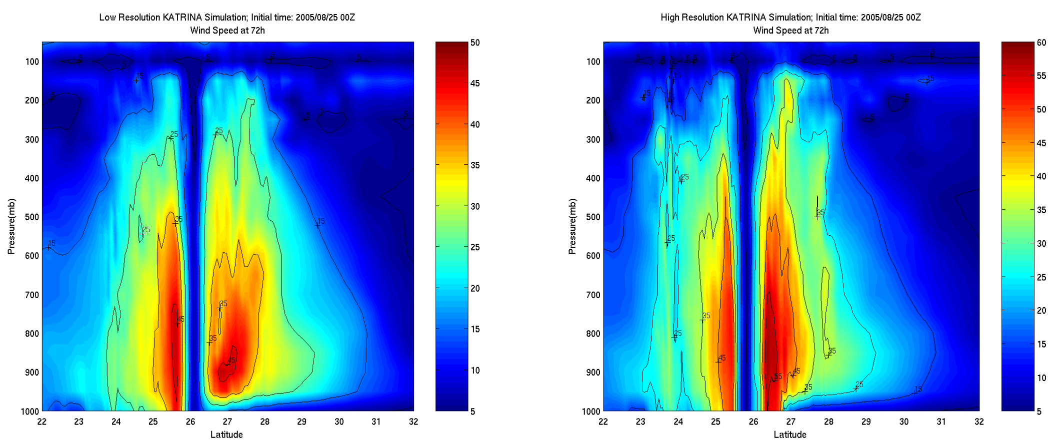

Figure 3. *Vertical-Zonal cross-sections of the wind speed at T=72 hours in Hurricane Katrina simulations initialized on Aug. 25, 00Z in the operational (left) and high-resolution (right) GFDN models.*

In these test experiments no changes in the model physics were made in the high-resolution model. It may be necessary to retune some of the parameters in the model physics in order to take full advantage of the better resolved inner-core structure with the higher resolution. More test experiments will be conducted during the second half of this year to evaluate the impact the high resolution on the hurricane forecast skill.

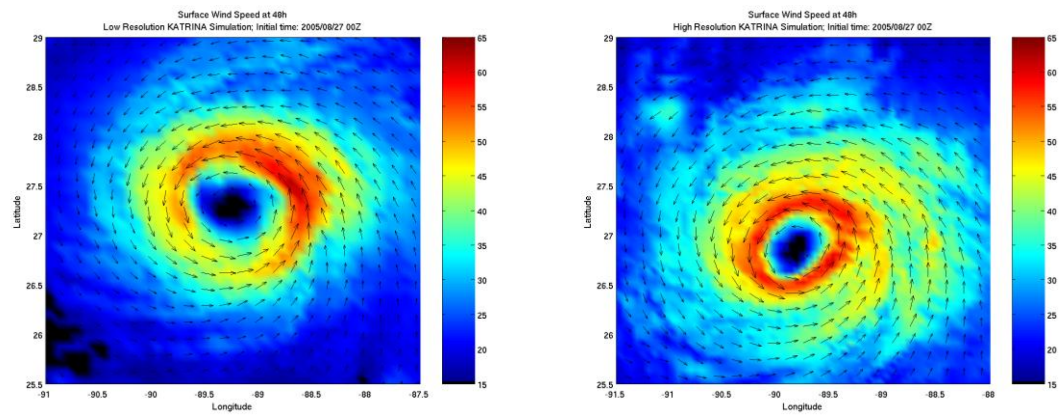

Figure 4. *Surface wind speed at T=72 hours in Hurricane Katrina simulations initialized on Aug. 25, 00Z in the operational (left) and high-resolution (right) GFDN models.*

b) GFDN-WAVEWATCH III coupling

The GFDN model has been successfully coupled with NOAA's WAVEWATCH wave model. The air-sea coupler has been redesigned to handle the wind-wave-current interaction processes. We are in the process of conducting idealized simulations in a hurricane embedded in specific environmental zonal flows of various strengths. Figure 5 shows surface wind, significant wave height, and energy dissipation at 72 hours in the simulation with a 5 m/s zonal flow. The asymmetries in the wave parameters relative to the storm center are clearly seen and consistent with observed patterns. We are in the process of conducting various sensitivity experiments to evaluate the impact of wave coupling and will present the results in the next report. The wave model performance for hurricane conditions has been extensively tested by Fan et al. (2009a).

c) Implementation of ASIM into HWRF

For both the HWRF and GFDN models, we are implementing new coupled modeling strategies that include the following: 1) in the hurricane model, the parameterizations of the air-sea heat and momentum fluxes and the spray source functions will explicitly include the sea state dependence and ocean currents; 2) the wave model will be forced by the sea-state dependent momentum flux and will include the ocean current effects; 3) the ocean model will be forced by the sea-state dependent momentum flux that accounts for the air-sea flux budget.

The key element of our coupled modeling strategy is the URI air-sea interface module (ASIM) shown in Fig. 6. ASIM consists of 1) the URI coupled wind-wave (CWW) boundary layer model of Moon et al. 2004 a,b (sub-module "MFLUX" in Fig. 6); 2) an air-sea energy and momentum flux budget model of Fan et al. 2009a and Fan et al. 2010 (sub-modules "MFBudget" and "WFlux" in Fig. 6) the NOAA/ESRL sea spray due to breaking waves model of Fairall et al. 2009 (sub-module "sea spray model" in Fig. 6). One of the novel features implemented in ASIM is the method of coupling between breaking waves and the NOAA/ESRL sea spray generation model. In the present NOAA/ESRL sea-spray model, the source function is parameterized in terms of energy lost to the wave breaking process, EF_c, which is simply related to the wind speed. The effective droplet source height h is related to the significant wave height. Within the framework of ASIM, the total energy lost to breaking (EF_c) is accurately estimated by explicitly accounting for the sea state dependence and the air-sea flux budget (Fan et al., 2010). The source height is determined not from the significant wave height but from the input wave age (wave age of the wind-forced part of the spectrum) and the wind stress. This modification is important under tropical cyclones because the dominant scale of breaking waves is related to the scale of the actively wind-forced waves – not related to the scale of swell generated elsewhere.

The ASIM will be embedded in GFDN and HWRF models and will calculate all the flux boundary conditions for the atmospheric, wave, and ocean models.

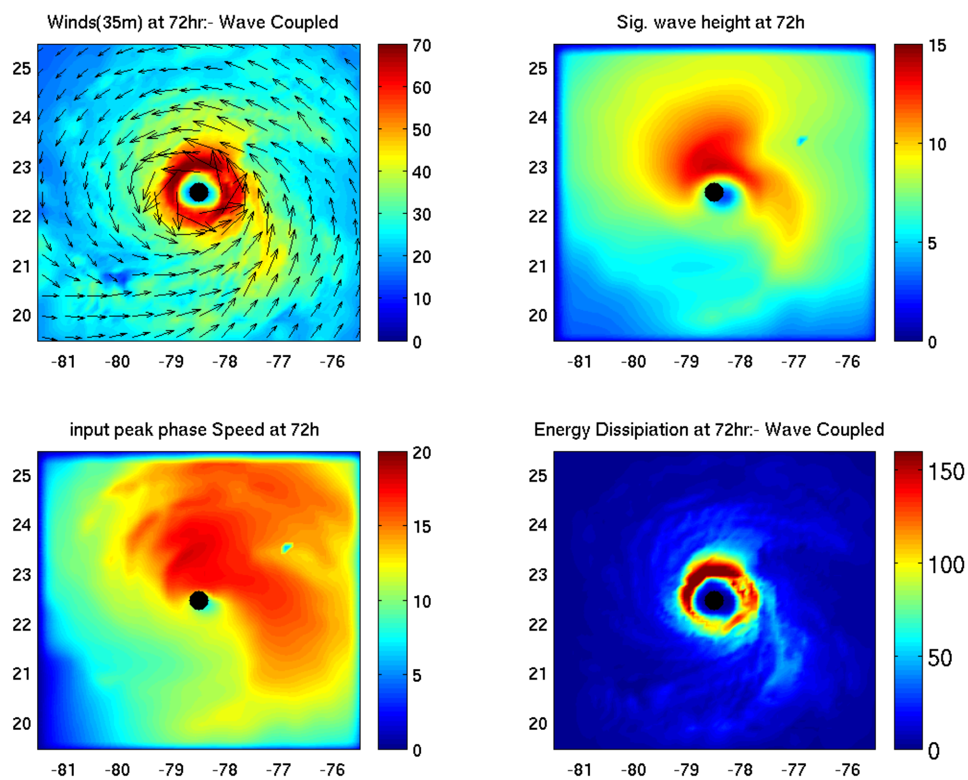

Figure 5. *Surface wind, significant wave height, peak phase speed and energy dissipation due to wave breaking at t=72 h in an idealized experiment using the GFDN coupled hurricane-wave-ocean system.*

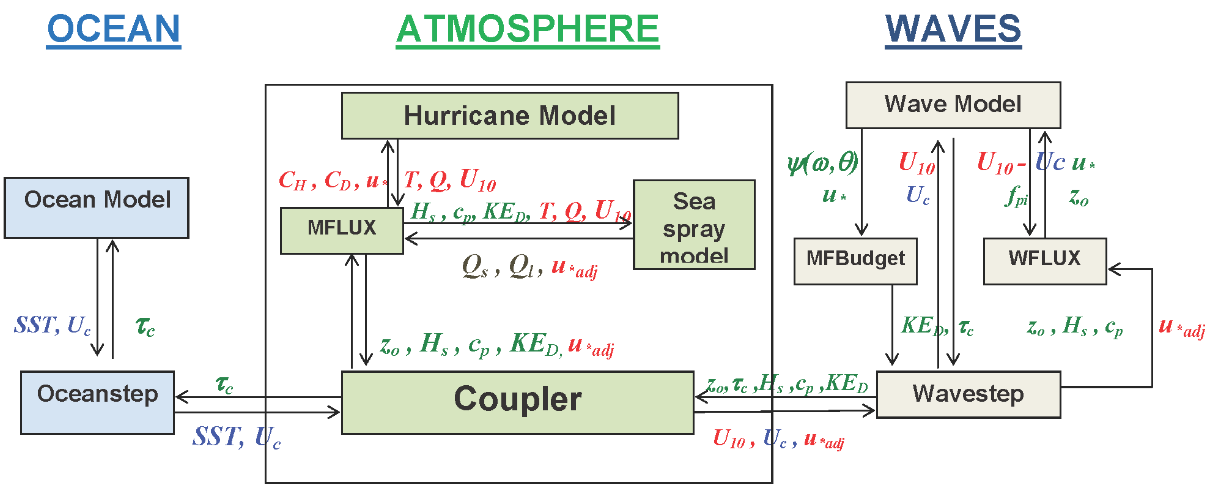

Figure 6. *A schematic diagram of the coupled wind-wave-current modeling system and the air-sea interface module (ASIM) represented by the following components: MFLUX, Sea spray model, MFBudget, and WFLUX. The arrows indicate the prognostic variables that are passed between the model components.*

References:

Fan, Y., I. Ginis, and T. Hara, 2010: Momentum flux budget across air-sea interface under uniform and tropical cyclones winds. *J. Phys. Oceanogr.*, in review.

Fan, Y., I. Ginis, T. Hara, C. W. Wright, and E. Walsh, 2009a: Numerical simulations and observations of surface wave fields under an extreme tropical cyclone. *J. Phys. Oceanogr.*, 39, 2097-2116.

Fan, Y., I. Ginis, and T. Hara, 2009b: The effect of wind-wave-current interaction on air-sea momentum fluxes and ocean response in tropical cyclones. *J. Phys. Oceanogr.*, 39, 1019-1034.

Fairall C. W., M. L. Banner, W. L. Peirson, W. Asher, R. P. Morison, 2009: Investigation of the physical scaling of sea spray spume droplet production. *J. Geophys. Res.*, **114**, C10001, doi:10.1029/2008JC004918.

Moon, I.-J., T. Hara, I. Ginis, S. E. Belcher, and H. Tolman, 2004a: Effect of surface waves on air–sea momentum exchange. Part I: Effect of mature and growing seas, *J. Atmos. Sci.*, **61**, 2321–2333.

Moon, I.-J., I. Ginis, and T. Hara, 2004b: Effect of surface waves on air–sea momentum exchange. II: Behavior of drag coefficient under tropical cyclones, *J. Atmos. Sci.*, **61**, 2334–2348.